Steel and Composite Structures, *Vol. 21, No. 6 (2016) 1265-1285*
DOI: http://dx.doi.org/10.12989/scs.2016.21.6.1265

Experimental investigation on shear capacity of RC beams with GFRP rebar & stirrups

Tarak P. Vora [*1] and Bharat J. Shah [2a]

[1] *PhD Department, Gujarat Technological University, Nr. Visat Three Roads, Visat - Gandhinagar Highway, Chandkheda, Ahmedabad – 382424, Gujarat, India*
[2] *Applied Mechanics Department, L. D. College of Engineering, No. 120, Circular Road, University Area, Opp. Gujarat University, Navrangpura, Ahmedabad – 380015, Gujarat, India*

(*Received March 24, 2016, Revised July 12, 2016, Accepted August 10, 2016*)

Abstract. This paper presents experimental results of advanced investigation carried out on the beams reinforced with Glass Fiber Reinforced Polymer (GFRP) rebar and stirrups. Twelve beams reinforced with GFRP and one beam with steel reinforcement of size 230 × 300 × 2000 mm were investigated. Longitudinal reinforcement, shear span and spacing of stirrups were the main variables to form the set. In advanced testing three types of strain gauges for steel, composite and concrete surface were applied to observe strain/stress development against the applied load. Live data were recorded from four strain gauges applied on stirrups, one at center on longitudinal reinforcement, two on the concrete surface and central deflection during the test. Although the focus of the paper was mainly on the behavior of GFRP shear reinforcement, other parallel data were observed for the completeness of the test. Design recommendations of ISIS Canada Design Manual (2007), Japan Society of Civil Engineers (1997) and American Concrete Institute (ACI-440.1R-06) were reviewed. Shear design predictions were compared with experimental results in which it was observed that all the three standards provided conservative predictions. However, ACI found most efficient compare to other two there is room to improve the efficiency of the recommendations.

Keywords: shear strength; reinforced concrete; glass fiber reinforced polymer; strain gauge; beams

1. Introduction

Service life of the structures has remained a great concern for the growing as well as the stable economy. Major cause of deterioration of the structure are corrosion of steel, fatigue, and increase in service loads, which in result produces the reduced life of the structures (Chen and Das 2009). With the advent of the technological revolution, it is equally important to explore and acknowledge the novel material to suit to the current state of affairs. Due to non-corrosive nature, different forms of FRPs have gained the acceptance as an alternative to the steel reinforcement. However, anisotropic, brittle elastic behavior, low modulus of elasticity, bend strength and bond characteristics make the FRPs different from steel reinforcement (Yost *et al*. 2001, Alam and Hussein 2013a, b, El Refai and Abed 2015). Even due to high strength and stiffness-to-weight ratio,

∗Corresponding author, Ph.D. Student, E-mail: vora.tarak@gmail.com
[a] Ph.D., E-mail: bjshah.ldce@gmail.com

http://www.techno-press.org/?journal=scs&subpage=6 ISSN: 1229-9367 (Print), 1598-6233 (Online)

FRPs have gain attraction in repair, retrofitting and strengthening of damaged structures also (Panda *et al*. 2013a, b). Glass Fiber Reinforced Polymer (GFRP) has no significant effect of harsh environmental condition of bond behavior (Al-Tamimi *et al*. 2014). Number of guidelines and standards are produced for the safe design using FRP reinforcement by; Intelligent Sensing for Innovative Structures, Canadian Network of Excellence (ISIS Canada 2007); Japan Society of Civil Engineering standard (JSCE 1997); International Federation for Structural Concrete standard (fib 2007); American Concrete Institute ; ACI 440.1R-06 (ACI 2006) and Canadian Standards Association standards CSA S6-06 and CSA S806-12 worldwide. Shear capacity has remained complex behavior. Shear failure of an RC beam is a type of failure mode that has a catastrophic effect and occurs with no advance warning of distress (Altin *et al*. 2011, Panda *et al*. 2012). Almost all the recommendations are following same format $V_r = V_c + V_s$, where total shear capacity (V_r) is the individual contribution of concrete (V_c) and stirrups (V_s). However, all the standards have adopted different approaches to derive individual contributions, which provide conservative results in overall.

Total five mechanisms for the concrete contribution (V_c) are reported by ACI-ASCE Committee 445 (1998) for the beams without shear reinforcement as shear resistance of (1) uncracked concrete in compression zone; (2) aggregate interlock; (3) residual tensile stress across the shear cracks; (4) dowel action; and (5) arch action. Variety of experimentation have been done on the FRP-reinforced concrete (FRP-RC) beams without shear reinforcement to evaluate V_c (Guadagnini *et al*. 2003, 2006, Tureyen and Frosch 2003, El-Sayed *et al*. 2006, Razaqpur and Isgor 2006, Steiner *et al*. 2008, Hoult *et al*. 2008, Jang *et al*. 2009, Alam and Hussein 2011, 2012, 2013a, b, Razaqpur and Saverio 2014), whereas limited experimentation is done to evaluate V_s on FRP-RC beams.

To quantify stirrups contribution V_s similar relationship in FRP-RC elements is used as for steel reinforced concrete elements just by changing the stress level at failure in almost all the current recommendations (Abed *et al*. 2012). Different recommendations provide limiting strain value for the FRP stirrups to avoid stirrup rupture in bent portion and to control crack width in the shear zone. It should be well noted that because of manufacturing process tensile strength and stiffness of stirrup (bent element) would be lower than the straight element manufactured with pultrution process (El-Sayed *et al*. 2007, Ahmed *et al*. 2010). Kinking of the innermost fibers would take place because of reduced strength of bend portion compare to straight portion. Collectively, bend strength is govern by manufacturing process, bend radius, bar diameter and type of reinforcing bar (ACI 2006).

In addition, it was observed that concrete contribution enhances after the formation of the first shear crack in FRP-RC elements. Even, lower spacing of FRP stirrups enhances the shear capacity due to confinement of concrete. This helps in improving aggregate interlock and also controls the shear cracks. The strain limit in FRP stirrups, as specified in different codes and guidelines, enables better, but still conservative, predictions of shear strength of concrete members reinforced with GFRP stirrups (Ahmed *et al*. 2010).

Permissible stain limits in the stirrups from 0.002 to 0.004 in different recommendations is one of the significant parameter to quantify the shear contribution in FRP-RC elements. The objective of the research to perform advanced testing on the beams (with different a/d ratio and spacing of stirrups) to provide experimental evidence which would facilitate to improve the efficiency of the current recommendations using FRP reinforcement.

2. Reseach significance

Researchers are confident that FRP is an alternative to the steel as a primary reinforcement in concrete members considering advantageous characteristics. Substantial research has been going on to improve the performance and efficiency in FRP reinforced concrete members. Shear performance of the FRP reinforced concrete members requires greater input from the researcher to understand well. Through the continuous efforts of the researchers, design recommendations for FRPs have been updated continuously; however, this area requires more concentration of the researchers to improve the efficiency. The objective of this research is to understand the shear performance of GFRP reinforced concrete members through advanced testing. Strain (indirectly stress) development in the GFRP shear and flexural reinforcement up to ultimate failure have been investigated and presented in this paper.

3. Review of the shear design recommendations

Traditionally, shear capacity of the reinforced concrete elements is evaluated as the addition of concrete and stirrups contributions with steel reinforcement; similarly it is followed for FRP reinforcement also. Majority of the design recommendations produced for FRP applications, conceptually replaces the steel reinforcement by FRPs with due modifications considering fundamental differences of the properties between them. Permissible stain approach in FRP stirrups is advisable to maintain the harmony and to control the shear crack width. This also helps to avoid failure of the FRP stirrups in the bent portion due to limited stress development (ACI 2006).

The shear strength contribution for concrete (V_c) and FRP reinforcement (V_{FRP}) as specified by the ISIS Canada (2007), JSCE (1997) and ACI (2006) are calculated as follows

$$V_r = V_c + V_{FRP} \tag{1}$$

3.1 ISIS Canada Design Manual (*2007*)

$$V_c = 0.2\lambda\Phi_c\sqrt{f'_c}b_w d\sqrt{\frac{E_{frp}}{E_s}} \leq 1 \qquad \text{where,} \qquad \sqrt{\frac{E_{frp}}{E_s}} \tag{2}$$

For the sections with an effective depth greater than 300 mm and not containing at least minimum transverse reinforcement the concrete resistance, V_c, is taken as

$$V_c = \left(\frac{260}{1000 + \mathrm{d}}\right)\lambda\varphi_c\sqrt{f'_c}b_w d\sqrt{\frac{E_{frp}}{E_s}} \qquad \text{where,} \qquad \sqrt{\frac{E_{frp}}{E_s}} \leq 1 \tag{3}$$

$$V_{FRP} = \varphi_{frp}\ \frac{A_{fv}\ \sigma_v d_v \cot\theta}{s} \tag{4}$$

$$\sigma_v = \frac{\left(0.05\frac{r_b}{d_b} + 0.3\right)f_{frpv}}{1.5} \tag{5}$$

$$\sigma_v = E_{frpb}\,\varepsilon_v \tag{6}$$

$$\varepsilon_{fv} = 0.0001\sqrt{f'_c \frac{\rho_{frp}\,E_{frp}}{\rho_{frpv}\,E_{frpv}}}\left[1 + 2\left(\frac{\sigma_N}{f'_c}\right)\right] \leq 0.0025 \tag{7}$$

3.2 JSCE (1997) Recommendations

The shear contribution of concrete as recommended is obtained as

$$V_c = \beta_d \beta_p \beta_n f_{cvd}\; bd \;/\; \gamma_b \tag{8}$$

$$f_{cvd} = 0.2(f'c)^{1/3} \leq 0.72 \text{ N /mm}^2 \tag{9}$$

$$\beta_d = (1000\;/\;d)^{1/4} \leq 1.5 \tag{10}$$

$$\beta_p = (100\,\rho_{fl} E_{fl}\;/\;E_s)^{1/3} \leq 1.5 \tag{11}$$

$$\beta_n = 1 + \frac{M_o}{M_d}, \qquad \text{if} \quad \beta_n > 2 \ \text{ or } N_f \geq 0 \tag{12}$$

$$\beta_n = 1 + \frac{2\,M_o}{M_d}, \qquad \text{if} \quad \beta_n < 0 \ \text{ or } N_f < 0 \tag{13}$$

The shear contribution by FRP stirrups is calculated as

$$V_{FRP} = [A_{fv}\; E_{fv}\; \varepsilon_{fv}\; (\sin\alpha s + \cos\alpha s)\;/\;s]\; z\;/\;\gamma_b \tag{14}$$

$$\varepsilon_{fv} = 0.0001\sqrt{f'_{mcd} \frac{\rho_{fl} E_{fl}}{\rho_{fv} E_{fv}}}\left[1 + 2\left(\frac{\sigma_N}{f'_{mcd}}\right)\right] \leq f_{FRPbend}\;/\;E_{fv} \tag{15}$$

$$f_{FRPbend} = \left(0.05\frac{r_b}{d_b} + 0.3\right) f_{fuv}\;/\;\gamma_{mfb} \tag{16}$$

$$f'_{mcd} = \left(\frac{\text{h}}{300}\right)^{-1/10} f'_{cd} \tag{17}$$

$$\sigma_N = N_f\;/\;A_g \leq 0.4\, f'_{mcd} \tag{18}$$

3.3 ACI 440.1R-06 (ACI 2006)

The shear resistance of concrete V_c in FRP-RC element specified by the ACI 440.1R-06 (ACI 2006) is as follows

$$V_c = \frac{2}{5}\sqrt{f'_c}\, b_w\, c \tag{19}$$

$$c = kd \tag{20}$$

$$k = \sqrt{2\,\sigma_f n_f + (\sigma_f n_f)^2} - \sigma_f n_f \tag{21}$$

The shear resistance of FRP stirrups VFRP of the member is calculated as

$$V_{FRP} = \frac{A_{fv}\sigma_{fv} d}{s} \tag{22}$$

$$\sigma_{fv} = 0.004E_{fv} \leq f_{FRPbend} \tag{23}$$

$$f_{FRPbend} = \left(0.05\frac{r_b}{d_b} + 0.3\right) f_{FRPu} \;/\; 1.5 \leq f_{FRPu} \tag{24}$$

4. Experimental investigation

4.1 Test specimens

Total thirteen real size beams were casted and investigated in this experimental study. Out of thirteen beams one was reinforced with steel while twelve beams were reinforced with GFRP including longitudinal and shear reinforcement. The beams with dimensional parameters of 230 mm wide, 300 mm height and total length of 2000 mm including 100 mm overhanging on each end were considered in the investigation. Total six combinations were developed by keeping

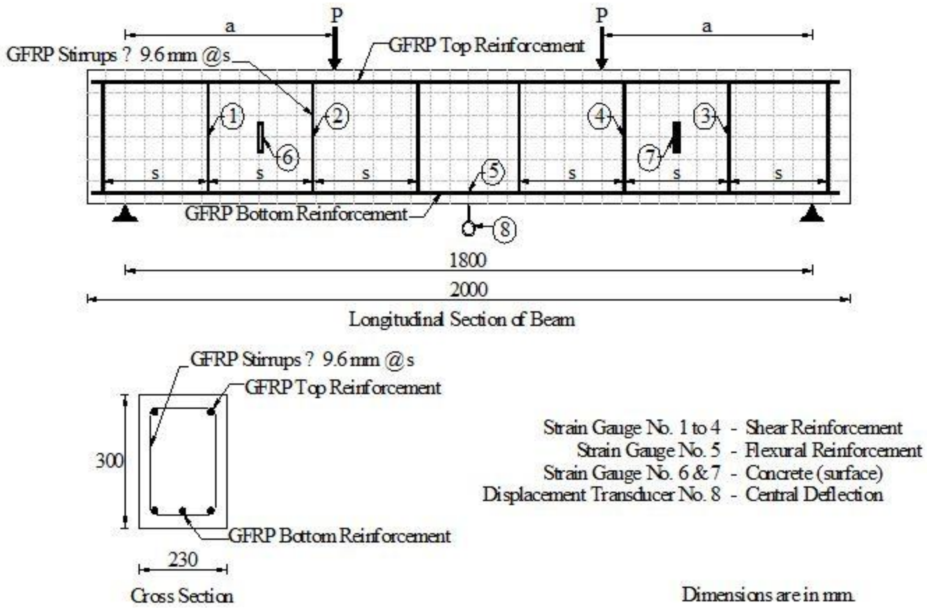

Fig. 1 Typical cross sectional details of beam

Table 1 Details of the flexural and shear reinforcement

Beam [a]	*a* (mm)	*a*/*d*	Top bars	Bottom bars	Stirrups dia. (mm)	*S* (mm)
SB.2.1	650	2.33	2-#10	3-#16	#8	275
GA.1.1 GA.1.2	500	1.79	2-Φ9.5	2-Φ18.71 + 1-Φ15.25	Φ9.5	250
GA.2.1 GA.2.2	500	1.79	2-Φ9.5	2-Φ18.71 + 1-Φ15.25	Φ9.5	275
GB.2.1 GB.2.2	650	2.33	2-Φ9.5	2-Φ18.71 + 1-Φ15.25	Φ9.5	275
GB.3.1 GB.3.2	650	2.33	2-Φ9.5	2-Φ18.71 + 1-Φ15.25	Φ9.5	300
GC.4.1 GC.4.2	750	2.69	2-Φ9.5	3-Φ18.71	Φ9.5	325
GC.5.1 GC.5.2	750	2.69	2-Φ9.5	3-Φ18.71	Φ9.5	350

[a] G$.%.N: G Type of Longitudinal and shear reinforcement (S : Steel and G : GFRP);
$ denotes distance "a", the location of two point load as per Fig. 1 (A = 500 mm, B = 650 mm, and C = 750 mm); % denotes spacing of shear reinforcement (1 = 250 mm, 2 = 275 mm, 3 = 300 mm, 4 = 325 mm and 5 = 350 mm),
N denotes serial number of the beam of that type.
# denotes tor steel reinforcement and Φ denotes GFRP reinforcement

Table 2 Physical properties of cement

Type of property	Experimental value	Value specified by IS 8112:1989
Standard consistency (%)	30.6	N/A
Fineness (m^2/kg)	314	225 (Min.)
Specific gravity	3.12	3.15
Setting time (Minutes)		
Initial	90	30 (Min.)
Final	175	600 (Max.)
Compressive strength (MPa)		
3 days	28.5	23 (Min.)
7 days	41.44	33 (Min.)
28 days	49.86	43 (Min.)

variation in shear span and spacing of shear reinforcement. Three variations in shear span-to-depth of 1.79, 2.33 and 2.69 were kept by providing shear span of 500 mm, 650 mm and 750 mm respectively. Total five variations in spacing were introduced in the spacing of stirrups like 250 mm, 275 mm, 300 mm, 325 mm and 350 mm with the aim to have different possible variation in shear behavior and ultimate strain condition in stirrups. Fig. 1 shows typical cross sectional details of the beam.

Table 3 Physical properties of coarse and fine aggregates

Property	Value obtained experimentally as per IS: 383-1970	
	Coarse aggregate	Fine aggregate
Type	Crushed	Natural
Maximum Size (mm)	20	4.74
Specific gravity	2.72	2.61
Water absorption (%)	0.78	0.71
Surface moisture (%)	Nil	0.9
Fineness modulus	5.12	2.78

All the six variations are designed as per ACI440.1R-06 where all the beams were reinforced with GFRP bars of average diameter of 15.25 mm and 18.71 mm in combination as per flexural reinforcement required, as mentioned in Table 1; while two 9.5 mm diameter GFRP bars were provided at top in longitudinal direction. In case of shear reinforcement 9.5 mm diameter GFRP bars with bent radius 45 mm was used with different spacing as stated and tabulated. However, beam with steel reinforcement was provided three 16 mm diameter bars at bottom and two 10 mm steel bars at top with stirrups of 8 mm diameter at an interval of 275 mm. details of the flexural and shear reinforcement are presented in Table 1.

4.2 Materials

All the specimens were cast in the Material Testing Laboratory of Marwadi Education Foundation's Group of Institutions, Gujarat, India using ready mixed concrete with a target compressive strength of 30 MPa at 28-days supplied by the Lafarge India Pvt. Ltd. Properties of raw materials like cement and aggregates (coarse and fine) are listed in Tables 2 and 3 respectively. All the beams were cast from the same batch and the actual properties of the concrete used were determined by testing of standard cubes 150 × 150 × 150 mm in compression on the testing day. Table 4 contains the concrete properties of test specimens.

GFRP reinforcement made of continuous longitudinal glass fibers impregnated in a thermosetting vinyl ester resin using infusion process with a average fiber content of 81.87% (by weight), manufactured by Dextra Group, were used as longitudinal and shear reinforcement. The GFRP reinforcement had a sand-coated surface to achieve improved bond performance with the surrounding concrete. Three different diameters 9.5 mm, 15.25 mm and 18.71 mm were used in

Table 4 Properties of concrete and GFRP reinforcement

Concrete		GFRP Reinforcement								
$f'c$ (Mpa)	E_c (Gpa)	d_b (mm)	Barcol hardness	Fibre content (%)	f'_{frpu} (Mpa)	E_{frp} (Gpa)	Ultimate strain	f'_{frpu} (Mpa)	E_{frp} (Gpa)	Ultimate strain
					Manufacturer Data			Experimental Results		
34.65	22.04	9.5	60	82.72	871	48.3	1.93	891	48.4	1.841
		15.25	62	82.64	904	48.2	2.05	911	48.2	1.89
		18.71	56	80.26	955	47.3	2.16	963	47.4	2.03

Fig. 2 GFRP bars and stirrup

longitudinal direction. The GFRP stirrups had a width 180 mm, overall depth 250 mm, and bend radius r_b 38 mm (4 times d_b). Photograph of GFRP bars and stirrups are shown in Fig. 2.

Based on the data supplied by the manufacturer M/s Dextra Group Limited different properties like fiber content, ultimate tensile strength, modulus of elasticity and ultimate strain of the GFRP bars of different diameters are listed in Table 4. Supplied parameters were derived as per the series of ASTM standards applicable for different parameters. The parameters like ultimate tensile stress, modulus of elasticity and ultimate strain were verified experimentally in the laboratory, where the values were very close to the provided data.

The tor steel bars of 16 mm and 10 mm diameter were used for bottom and top reinforcement respectively, while in case of shear reinforcement 8 mm diameter stirrups were used. Based on test

Table 5 Mechanical properties of steel reinforcement

Type of reinforcement	Nominal diameter (mm)	Yield stress (MPa)	Ultimate stress (MPa)	Elongation (%)	Reduction in area (%)
Tor steel	16	451.45	578.9	20.08	43.55
Tor steel	10	449.35	583.48	19.32	46.32
Tor steel	8	461.59	575.82	19.63	44.83

(a) FLA-3-11-1L (b) PL-90-11-3L (c) BFLA-5-5-3L

Fig. 3 Types of strain gauges

results of three steel specimens, the average yield stress and modulus of elasticity were 454 MPa and 200 GPa, respectively. Table 5 contains the mechanical properties of steel reinforcement.

4.3 Instrumentation

To observe strain on the reinforcement and concrete, strain gauges manufactured by Tokyo Sokki Kenkyujo Co. Ltd. (TML), Japan were used. Four strain gauges on the shear reinforcement in the shear zone on either side, one on flexural reinforcement at mid-span and two on the concrete surface in the shear crack zone on either side were applied for the strain measurement. Specific strain gauges like PL-90-11-3L (Gauge length 90 mm, Gauge factor 2.10 ± 1%, Resistance 119.90 ± 0.5 Ω) for concrete (surface), BFLA-5-5-3L (Gauge length 5 mm, Gauge factor 2.09 ± 1%, Resistance 120.4 ± 0.5 Ω) for composite reinforcement (GFRP) and FLA-3-11-1L (Gauge length 2 mm, Gauge factor 2.10 ± 1%, Resistance 120.4 ± 0.5 Ω) for steel were used to observe the strain. Specific adhesive type CN for reinforcement and type CN-E for concrete were used to paste the strain gauge supplied by TML. Fig. 3 shows the types of strain gauges.

The mid-span deflection of the beam was measured using displacement transducers CDP – 100 (TML). The development of shear crack was observed till first crack appeared, immediately after strain gauges for concrete application (PL-90-11-3L) were pasted over the shear crack oriented perpendicular to the crack developed. The width of the shear crack observed visually was measured with high accuracy microscope. Detailed observation of the shear crack development and propagation were recorded during the test.

4.4 Test setup and procedure

All the beams were tested in four-point bending over a simply supported clear span of 1,800 mm in loading frame of capacity 550 kN. The load was monotonically applied approximately up to 90% of the expected failure load using hydraulic jack connected to the frame with a controlled rate of 5 kN/min. Thereafter, to reduce the accidental chances because of brittle shear failure, the load applied was displacement-controlled at a rate of 0.6 mm. Data acquisition system TMR-200 from Tokyo Sokki Kenkyujo Co, Ltd. was used to record strain in reinforcement and concrete as well as central deflection. Same was connected to computer also to store the data observed in dual mode. The complete test setup is shown in Fig. 4.

Fig. 4 Test setup

5. Results and discussion

The summary of the test results regarding the shear capacity of test specimens, maximum strains, angle of the major shear crack, and mode of failure are summarized in Table 6. However, detailed analysis and discussion of the results will be introduced through this section.

5.1 Capacity and mode of failure

As per the research objective all the test specimens reinforced with steel and GFRP reinforcement were designed to fail in shear. Hence, the ultimate failure of the entire test specimen was governed by the stirrup contribution. The entire sample was grouped in three major categories A, B & C by a/d ratio 1.79, 2.33 and 2.69 respectively and subgroups 1, 2, 3, 4 and 5 by spacing of stirrups 250, 275, 300, 325 and 350 mm respectively. Major difference in load level was observed as per a/d ratio while spacing of stirrups made marginal difference. All the beams failed with similar mechanism; however, the load levels of different categories were different. Sudden failure occurred due to diagonal tension cracks and rupture of GFRP stirrups. GFRP stirrups ruptured at the bend initially; subsequently, beams failed as other shear resisting mechanisms could not resist the shear force applied. This was because the flexural strength provided was greater than the shear strength of the beams. The groups A, B and C of the test specimens reinforced with GFRP failed at

(a). GA.1.1

(b). GA.1.2

(c). GA.2.1

(d). GA.2.2

(e). GB.2.1

(f). GB.2.2

Fig. 5 Failure of test specimens

(g). GB.3.1

(h). GB.3.2

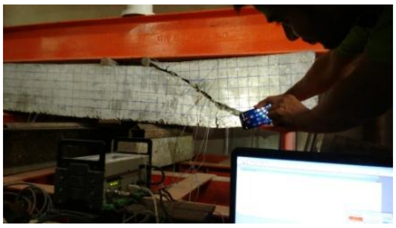

(i). GC.4.1

(j). GC.4.2

(k). GC.5.2

(l). GC.5.2

Fig. 5 Continued

average shear of 110 kN, 78 kN and 58 kN respectively. While the beam SB.2.1 reinforced with steel failed at applied shear of 91 kN by stirrups yielding and consequently diagonal tension failure of concrete. Failed specimens showing crack pattern and failure plane are shown in Fig. 5. The test specimens showed similar cracking pattern and inclination angle. However, the difference was in the total number of diagonal cracks appeared in the shear span and consequently their spacing. The higher the failure load the higher the number of shear cracks.

5.2 Load – deflection relationship

All the thirteen beam specimens one of steel and other twelve of GFRP reinforcement failed in shear prior to reaching their flexural capacity. Hence, brittle failure was observed in all the beams. Displacement transducer CDP-100 (TML, Japan) was used to observe the central deflection which was connected to TMR-200 to record online deflections. Deflection observed at failure load 126.46 kN in controlled beam SB.2.1 is 13.8 mm. Where in case of GFRP reinforced beam, maximum and minimum deflections observed are 23.96 mm at 118.49 kN and 12.28 mm at 69.7 kN in GB.3.1 and GA.1.1 respectively. The average deflection of all the beams observe is 17.68 mm at the average load of 130.88 kN. The relationships of applied shear force-Central deflection of all tested beams are shown in Fig. 6. The entire specimens with GFRP reinforcement showed similar behaviour; no significant difference observed between the beams with different spacing of

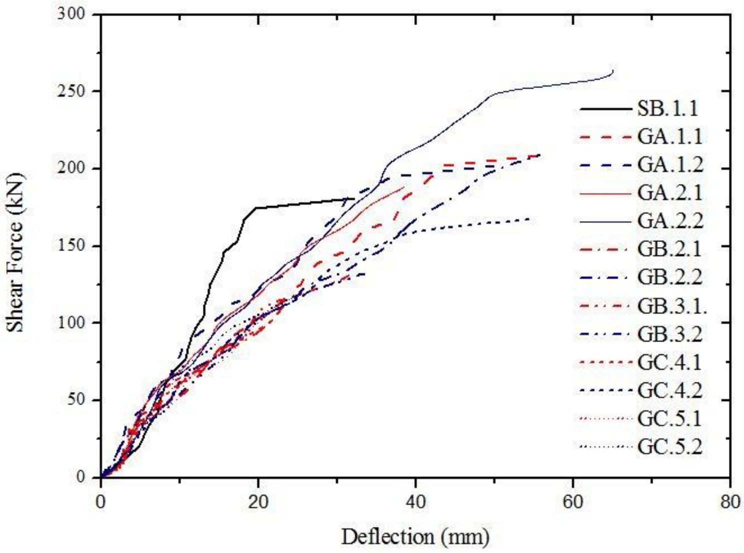

Fig. 6 Shear force – Midspan deflection relationship of all beam specimens

GFRP stirrups. However, the control beam reinforced with steel stirrups showed lesser deflection compare to GFRP. Thus, the variation in spacing or reinforcement material did not have a significant effect on the central deflection of all test specimens.

5.3 Load – crack width relationship

As the FRP is noncorrosive material by nature, allowable crack width would be to justify the aesthetics of the structure as protection to the reinforcement is not significant as in case of steel. However, specified limit for shear crack width is 0.5 mm in few standards. PL-90-11-3L type of concrete surface strain gauges were applied in the perpendicular direction of the shear crack in each shear zone of the beam as specified in Fig. 1. Diagonal tension along the crack would act as an axial tension in the concrete strain; hence, strain developed will provide the crack width over the surface indirectly. Fig. 7 shows the measured crack width formed diagonally in the shear zone where failure taken place against the applied shear force of all the test specimens. In the first group of shear span 500 mm, GA.1.2 observe 0.5 mm crack width at shear force of 139.4 kN where other beams GA.1.1, GA.2.1 and GA.2.2 have observed at 146.37 kN. In second group of shear span 650 mm, beams GB.2.1, GB.2.2, GB.3.1and GB.3.2 observed the 0.5 mm crack width at 104.55 kN, 111.52 kN, 118.49 kN and 111.52 kN respectively. Whereas, in third group of shear span 750 mm, beams GC.4.1, GC.4.2, GC.5.1and GC.5.2 observed the 0.5 mm crack width at 90.61 kN, 111.52 kN, 104.55 kN and 111.52 kN respectively.

Beams with smaller stirrups spacing exhibited cracks at larger load as compared to their counterparts with larger spacing of stirrups. The average strain observed in the stirrups at 0.5 mm crack width is 4712 microstrain which higher than the limits specified in any of the standard.

5.4 Flexural strains on GFRP longitudinal reinforcement

FLA type strain gauge was used to observe flexural strains on longitudinal reinforcement at location No. 5 as shown in Fig. 2. Average flexural strains developed in longitudinal reinforcement at design load were 1343, 1920 and 3633 microstrain observed at the average shear force of 197.77 kN, 158.56 kN and 142.88 kN respective to load positions “a” equals to 500 mm, 650 mm and 750 mm. Even the variation in strain development at design load as well as at ultimate load was observed; as the effective depth of corner and central reinforcement due to bend radius rb provided in stirrups were different. The average ultimate strains developed were 8137 and 5781 in central and corner reinforcement respectively. The relationships of shear force and flexural strain in longitudinal reinforcement at midspan of all beams are shown in Fig. 8.

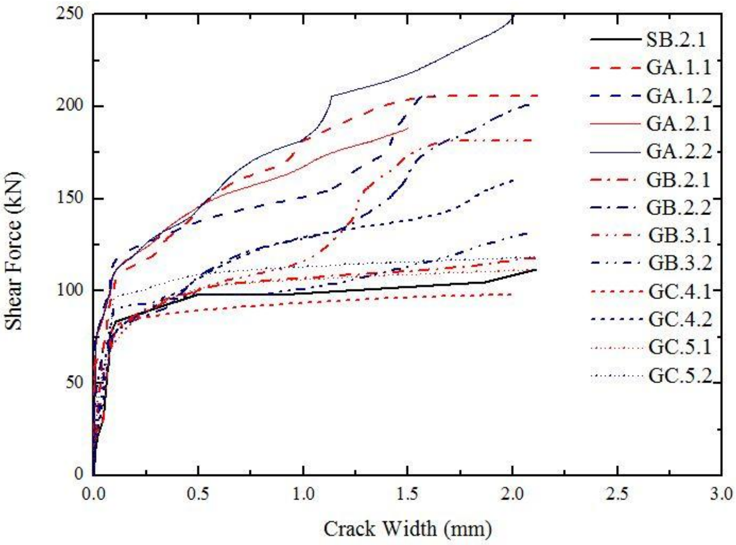

Fig. 7 Shear force – Crack width relationship of all beam specimens

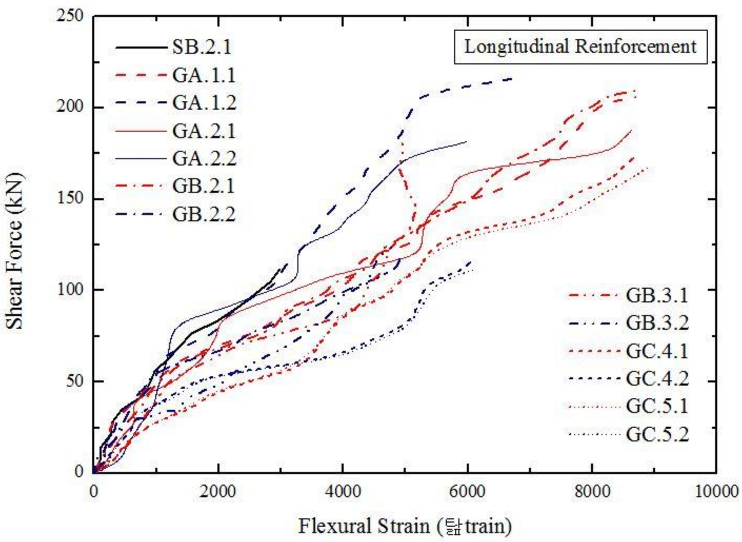

Fig. 8 Shear force – Flexural strain on longitudinal reinforcement relationship at midspan

5.5 Concrete surface strains

The preliminary use of concrete strain gauge was to observe crack width over the concrete surface. All the beams designed were shear deficit; hence, the expected failure was in shear. PL type strain gauge was applied on the concrete surface in the shear zone area where the shear crack was expected at location No. 6 and 7 as per Fig. 2. Maximum strain observed through concrete strain gauge was 23516 microstrain after that the strain gauges were failed. The relationships of shear force and concrete strain for the locations were shear failure occurred in all the beams, are shown in Fig. 9.

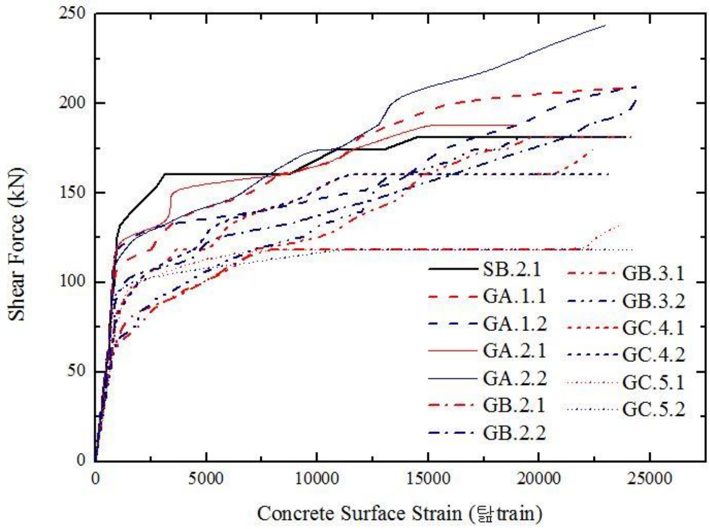

Fig. 9 Shear force – Concrete surface strain relationship of all beam specimens

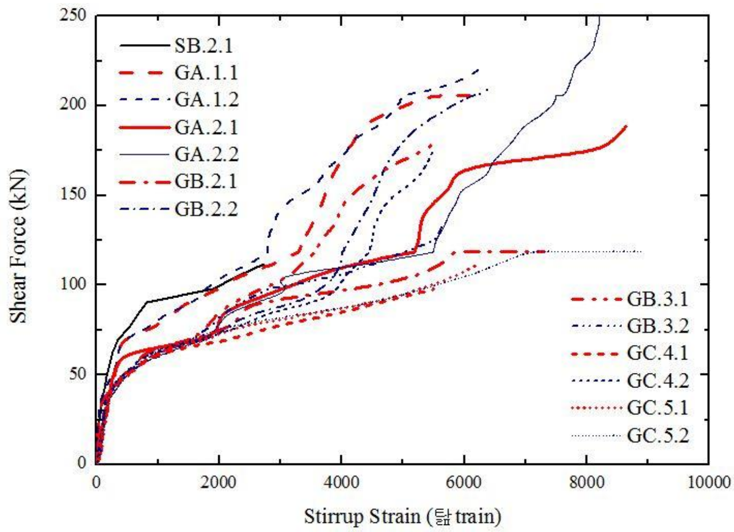

Fig. 10 Shear force – Stirrup strain relationship of all beam specimens

5.6 Strains on GFRP stirrups

Total four FLA type strain gauges on the straight portion of the GFRP stirrups symmetrically two in each of the shear zone area of the beam were applied as shown in Fig. 1. The relationships of applied shear-stirrup strain of all the beams are shown in Fig. 10. In the first group of shear span 500 mm, strain observed on stirrups at 0.5 mm crack width in the beams GA.1.1, GA.1.2, GA.2.1 and GA.2.2 are 3689, 2946, 5506 and 5890 microstrain at 146.37 kN, 139.4 kN, 146.37 kN and 146.37 kN, In second group of shear span 650 mm, stirrups strain in the beams GB.2.1, GB.2.2, GB.3.1and GB.3.2 are 5184. 3987, 3578 and 4522 microstrain at 104.55 kN, 111.52 kN, 118.49 kN and 111.52 kN respectively. Whereas, in third group of shear span 750 mm, beams GC.4.1, GC.4.2, GC.5.1and GC.5.2 have observed 4639, 4246, 5820 and 6534 microstrain at 90.61 kN, 111.52 kN, 104.55 kN and 111.52 kN respectively. The average maximum strain in GFRP stirrup observed was 6705 microstrains with a maximum strain of 8936 microstrains in the cases where stirrups failure occurred. These measured strains are approximately 1.76 and 2.68 times higher than the strain specified by ACI-2006 (4000 microstrain) and ISIS Canada-2007 (2500 microstrain) respectively. Corresponding stress produced in the straight portion of the stirrups is 36.40% of the ultimate strength of the stirrups; whereas the bend strength of the stirrups is 16.58% higher with respect to current permissible strain value as per ACI recommendations, which is yet conservative.

Small strain value for steel beam of 2726 microstrain at 111.52 kN was attributed to the fact that the strain in steel remains lower than the GFRP. It can also be seen that the stirrup strain

Table 6 Shear prediction, performance and failure of GFRP reinforcement

Beam	Shear crack load [a] V_{cr} (kN)	Ultimate shear V_{Exp} (kN)	Angle of major crack, θ (Degree)	Maximum stirrups strain (μstrain)	Mode of failure [b]	V_{Exp}/V_{Pred}		
						ISIS 2007	JSCE 1997	ACI 2006
SB.2.1	40.08	55.76	45	2726	ST	--	--	--
GA.1.1	54.02	102.81	49	6189	DT	2.72	2.23	1.86
GA.1.2	59.25	111.52	49	6363	DT	2.57	2.11	1.76
GA.2.1	54.02	94.10	46	8642	SR	2.84	2.30	2.00
GA.2.2	55.76	130.69	47	8204	DT	2.85	2.30	2.00
GB.2.1	34.85	59.25	46	6386	SC	1.96	1.58	1.38
GB.2.2	38.34	104.55	49	7312	SC	2.17	1.76	1.53
GB.3.1	34.85	90.61	47	5578	SC	2.00	1.60	1.44
GB.3.2	45.31	66.22	45	5634	SR	1.93	1.54	1.39
GC.4.1	45.31	49.49	39	5499	ST	1.94	1.49	1.41
GC.4.2	38.34	66.22	42	5488	ST	2.14	1.64	1.55
GC.5.1	34.85	55.76	45	6228	ST	2.16	1.65	1.59
GC.5.2	48.79	59.25	45	8936	ST	2.18	1.66	1.61
					Average	2.29	1.82	1.63
					SD	0.36	0.31	0.23

[a] Derived from the changing slope of the applied shear-concrete strain relationship as well as strain gauge readings.

[b] ST = Shear Tension, DT = Diagonal Tension, SR = Stirrups Rupture and SC = Shear Compression

increases with the spacing of stirrups as the stirrups contribution increases with the spacing. It is worth mentioning that testing was done with controlled rate of loading and considered details are of location where shear failure was occurred. In general, the stirrups strains remained very small until diagonal cracks were developed; then, rapid increase in the strain was observed until failure. Details relevant to shear failure like shear crack load, ultimate shear, shear crack angle, maximum stirrup strain and type of failure are represented in Table 6.

5.7 Comparison of experimental and predicted shear strength

Table 6 also presents a comparison between the experimentally measured shear capacity and the predicted ones. It can be observed from the Table 6 that shear provisions in both the standards ISIS Canada (2007) and JSCE (1997) greatly underestimate the shear strength while ACI (2006) predicts reasonable capacity which is yet conservative. This is referred to the common concept in calculating the concrete contribution (V_c) and FRP stirrup contribution (V_{FRP}) separately to derive shear capacity of the beam.

The least stirrups strength derived from bend strength from Eq. (5) and the value from Eq. (6) are used by ISIS Canada (2007). Here, Eq. (6) governs the design which remains well below compare to actual stress in the stirrups. The calculated average ratio of shear capacity experimental to the predicted (V_{Exp}/V_{Pred}) is 2.29 with standard deviation (SD) 0.36. Where, JSCE (1997) has kept the bend strength as the upper limit; however, the value used in design given by Eq. (15) governs the stirrups capacity which also remains very low compare to actual one. Here, the same average ratio V_{Exp}/V_{Pred} is 1.82 with SD 0.31, which quite lesser than the ISIS Canada. In case of ACI (2006) the average ratio V_{Exp}/V_{Pred} is 1.63 with SD 0.23. ACI (2006) uses constant strain value as an upper limit to predict the shear capacity, which is quite reasonable in comparison, however, yet conservative.

6. Conclusions

The experimental behavior and shear strength obtained through the advanced testing of the beams reinforced with GFRP longitudinal and lateral reinforcement are presented and discussed. The main variables were shear span to depth ratio and spacing of the shear reinforcement (stirrup). Sand-coated GFRP stirrups of 9.5 mm diameter were used as shear reinforcement with different spacing. The experimental test results were compared to the shear design provisions provided by ISIS Canada (2007), JSCE (1997) and ACI (2006). The main findings of this investigation can be summarized as follows:

- In the FRP-RC beams, GFRP stirrups as shear reinforcement did not affect the failure mechanism as a beam action in all the beams. Initial hair crack in flexure and consequently shear failure happened in all the beams.
- Strain development started at the initial stage of loading in case of higher spacing of stirrups compare to lower spacing. However, spacing did not affect the ultimate strain developed in the stirrups.
- Due to collective effect of shear span to depth ratio, cross section of beam, amount of shear and anchorage reinforcement, groups with shear span to depth ratio 1.79, 2.33 and 2.69 failed in diagonal tension, shear compression and shear tension in majority respectively.
- The average maximum strain in GFRP stirrup observed was 6705 microstrains with a

maximum strain of 8936 microstrains in the cases where stirrups failure occurred. The average strain observed in the stirrups at 0.5 mm crack width is 4712 microstrain which higher than the limits specified in any of the standard.

- Crack angle of the failed specimens varied from 39° to 49° with an average of around 45°, which shows good agreement with traditional truss model.
- Shear capacity predicted by ISIS Canada (2007) is the most conservative with the ratio V_{Exp}/V_{Pred} as 2.29 out of three. Both the contributions concrete and shear are underestimated by this standard. There is no point in calculating concrete contribution by considering steel as the reference material. Permissible strain value 0.0025 is also very low compare to actual values as well as 0.004 as used by ACI (2006).
- JSCE (1997) also gives the conservative prediction with the ratio V_{Exp}/V_{Pred} as 1.82. Keeping the bend strength as upper limit is reasonable but Eq. (15) underestimates the strain value to be considered.
- ACI (2006) have shown good agreement with the ratio V_{Exp}/V_{Pred} as 1.63 which is yet conservative. Initially ACI-440.1R-03 had proposed permissible strain value as 0.002 similar to the steel reinforcement. This has been revised in ACI-440.1R-06 as 0.004 considering the linear elastic behavior and ultimate strain value of FRPs. There is room to increase the strain limit to improve the efficiency of the recommendations.
- As average strain on stirrups is 4712 and maximum strain is 5890 at 0.5 mm crack width, if permissible strain is increased to 0.005, the average ratio V_{Exp}/V_{pred} and SD reduces to 1.45 from 1.63 and 0.2 from 0.23 respectively.

Acknowledgments

The researchers wish to express their gratitude and sincere appreciation to the Marwadi Education Foundation's Group of Institution, India for financing this research work. The researchers would like to pay their gratitude to the technical staff in the structural laboratory and post graduate students at the Department of Civil Engineering for their assistance in fabricating and testing the specimens.

References

Abed, F., El-Chabib, H. and AlHamaydeh, M. (2012), "Shear characteristics of GFRP-reinforced concrete deep beams without web reinforcement", *J. Reinforced Plastics Compos*., **31**(16), 1083-1073.

ACI 318-11 (2011), Building code requirements for structural concrete and commentary, American Concrete Institute, Farmington Hills, MI, USA.

ACI 440.1R-06 (2006), Guide for the design and construction of concrete reinforced with FRP bars, American Concrete Institute, Farmington Hills, MI, USA.

Ahmed, E., El-Salakawy, E. and Benmokrane, B. (2010), "Shear performance of RC bridge girders reinforced with carbon FRP stirrups", *J. Bridge Eng*., **15**(1), 44-54.
DOI: 10.1061/(ASCE)**BE**.1943-5592.0000035

Alam, M.S. and Hussein, A. (2011), "Experimental investigation on the effect of longitudinal reinforcement on shear strength of fibre reinforced polymer reinforced concrete beams", *Can. J. Civil Eng*., **38**(3), 243-251.

Alam, M.S. and Hussein, A. (2012), "Effect of member depth on shear strength of high-strength fiber-reinforced polymer-reinforced concrete beams", *J. Compos. Construct*., **16**(2), 119-126.

DOI: 10.1061/(ASCE)**CC**.1943-5614.0000248

Alam, M.S. and Hussein, A. (2013a), "Size effect on shear strength of FRP reinforced concrete beams without stirrups", *J. Compos. Construct.*, **17**(4), 507-516. DOI: 10.1061/(ASCE)**CC**.1943-5614.0000346

Alam, M. S., and Hussein, A. (2013b), "Unified shear design equation for concrete members reinforced with fiber–reinforced polymer without stirrups", *J. Compos. Construct.*, **17**(5), 575-583. DOI: 10.1061/(ASCE)**CC**.1943 -5614.0000342

Al-Tamimi, A., Abed, F.H. and Al-Rahmani, A. (2014), "Effects of harsh environmental exposures on the bond capacity between concrete and GFRP reinforcing bars", *Adv. Concrete Construct.*, **2**(1), 1-11.

Altin, S., Anil, O. and Kara, M.E. (2011), "Retrofitting of shear damaged RC beams using CFRP strips", *Steel Compos. Struct., Int. J.*, **11**(3), 207-223.

ASCE-ACI Committee 445 on Shear and Torsion (1998), "Recent approaches to shear design of structures", *J. Struct. Eng.*, **12**(1375), 1375-1417. DOI: 10.1061/ (ASCE)0733-9445(1998)124

Chen, M. and Das, S. (2009), "Experimental study on repair of corroded steel beam using CFRP", *Steel Compos. Struct., Int. J.*, **9**(2), 103-118.

El Refai, A. and Abed, F. (2015), "Concrete contribution to shear strength of beams reinforced with basalt fiber-reinforced bars", *J. Compos. Construct.*, 04015082-1-04015082-13. DOI: 10.1061/(ASCE)CC.1943-5614.0000648

El-Sayed, A.K., El-Salakawy, E.F. and Benmokrane, B. (2006), "Shear strength of FRP-reinforced concrete beams without transverse reinforcement", *ACI Struct. J.*, **103**(2), 235-243.

El-Sayed, A.K., El-Salakawy, E. and Benmokrane, B. (2007), "Mechanical and structural characterization of new carbon FRP stirrups for concrete members", *J. Compos. Construct.*, **11**(4), 352-362.

Guadagnini, M., Pilakoutas, K. and Waldron, P. (2003), "Shear performance of FRP reinforced concrete beams", *J. Reinf. Plast. Compos.*, **22**(15), 1389-1407.

Guadagnini, M., Pilakoutas, K. and Waldron, P. (2006), "Shear resistance of FRP RC beams: Experimental study", *J. Compos. Constr.*, **10**(6), 464-473. DOI: 10.1061/ (ASCE)1090-0268(2006)**10:6**(464)

Hoult, N.A., Sherwood, E.G., Bentz, E.C. and Collins, M.P. (2008), "Does the use of FRP reinforcement change the one-way shear behavior of reinforced concrete slabs", *J. Compos. Construct.*, **12**(2), 125-133. DOI: 10.1061/(ASCE) 1090-0268(2008)**12:2**(125)

Intelligent Sensing for Innovative Structures (2007), Reinforcing concrete structures with fiber reinforced polymers, ISIS Canada, University of Winnipeg, Winnipeg, MB, Canada.

Jang, H., Kim, M., Cho, J. and Kim, C. (2009), "Concrete shear strength of beams reinforced with FRP bars according to flexural ratio and shear span to depth ratio", *Proceedings of the 9th International Conference Fiber Reinforced Polymer for Reinforced Concrete Structures*, American Concrete Institute, Sidney, Australia, July.

Japan Society of Civil Engineering (1997), Recommendation for design and construction of concrete structures using continuous fiber reinforcing materials, Tokyo, Japan.

Panda, K.C., Bhattacharyya, S.K. and Barai, S.V. (2012), "Shear behaviour of RC T-beams strengthened with U-wrapped GFRP sheet", *Steel Compos. Struct., Int. J.*, **12**(2), 149-166.

Panda, K.C., Bhattacharyya, S.K. and Barai, S.V. (2013a), "Shear strengthening effect by bonded GFRP strips and transverse steel on RC T-beams", *Struct. Eng. Mech., Int. J.*, **47**(1), 75-98.

Panda, K.C., Bhattacharyya, S.K. and Barai, S.V. (2013b), "Effect of transverse steel on the performance of RC T-beams strengthened in shear zone with GFRP sheet", *Construct. Build. Mater.*, **41**, 79-90.

Razaqpur, A.G. and Isgor, O.B. (2006), "Proposed shear design method for FRP-reinforced concrete members without stirrups", *ACI Struct. J.*, **103**(6), 93-102.

Razaqpur, A.G. and Spadea, S. (2014), "Shear strength of FRP reinforced concrete members with stirrups", *J. Compos. Constr.*, 04014025-(1-15). DOI: 10.1061/(ASCE)**CC**.1943-5614.0000483

Steiner, S., El-Sayed, A.K., Benmokrane, B., Matta, F. and Nanni, A. (2008), "Shear behaviour of large-size beams reinforced with glass FRP bars", *Proceedings of the 5th International Conference on Advanced Composite Materials in Bridges and Structures*, Winnipeg, Manitoba, Canada, September.

Tureyen, A.K. and Frosch, R.J. (2003), "Concrete shear strength: Another perspective", *ACI Struct. J.*,

100(5), 609-615.
Yost, J.R., Gross, S.P. and Dinehart, D.W. (2001), "Shear strength of normal strength concrete beams reinforced with deformed GFRP bars", *J. Compos. Construct.*, **5**(4), 268-275.

CC

Nomenclature

The following symbols are used in this paper:

A_{fv}	=	total cross-sectional area of shear reinforcement (mm^2);
A_g	=	total cross-sectional area of the member (mm^2);
A_s	=	area of cross section of steel or FRP reinforcing bars (mm^2);
b	=	beam width (mm);
c	=	neutral axis depth (mm);
d	=	distance from extreme comp. fiber to centroid of tension r/f (mm);
d_b	=	bar diameter (mm);
d_v	=	effective shear depth for longitudinal reinforcement (mm);
E_{fl}	=	modulus of elasticity of longitudinal reinforcement (MPa);
E_{fv}	=	modulus of elasticity of the shear reinforcement (MPa);
E_s	=	modulus of elasticity of steel (MPa);
f_c	=	compressive strength of the concrete (MPa);
f_{cr}	=	cracking strength of the concrete (MPa);
$f_{FRPbend}$	=	strength of bent portion of FRP bar (MPa);
f_{FRPu}	=	design tensile strength of FRP (MPa);
f_{fuv}	=	tensile strength of the straight portion of the shear reinforcement (MPa);
f_{mcd}	=	design compressive strength of concrete allowing for size effect (MPa);
h	=	total depth of the member (mm);
M_d	=	design bending moment (N/mm);
M_f	=	factored moment at a section (N/mm);
M_o	=	decompression moment (N/mm);
N_f	=	factored axial load occurring simultaneously with V_f (N);
n_f	=	modular ratio;
r_b	=	internal bend radius of the FRP stirrups (mm);
s	=	spacing of shear reinforcement (mm);
s_z	=	crack spacing parameter;
s_{ze}	=	equivalent crack spacing parameter; shall not be taken less than $0.85s_z$;

V_c	=	factored shear resistance provided by tensile forces in concrete (N);
V_f	=	factored shear force at a section (N);
V_{FRP}	=	factored shear resistance provided by the FRP shear reinforcement (N);
V_r	=	factored shear resistance (N);
α_s	=	angle between the shear reinforcement and axis of the beam;
β	=	actor used to account for the shear resistance of cracked concrete;